A&A 409, 563–571 (2003)
DOI: 10.1051/0004-6361:20031082

Astronomy & Astrophysics

Variation of cosmic ray injection across supernova shocks

H. J. Völk[1], E. G. Berezhko[2], and L. T. Ksenofontov[2,3]

[1] Max-Planck-Institut für Kernphysik, Postfach 103980, 69029 Heidelberg, Germany
e-mail: Heinrich.Voelk@mpi-hd.mpg.de
[2] Institute of Cosmophysical Research and Aeronomy, 31 Lenin Ave., 677891 Yakutsk, Russia
e-mail: berezhko@ikfia.ysn.ru
[3] Institute for Cosmic Ray Research, University of Tokyo, Kashiwa, Chiba 277-8582, Japan
e-mail: ksenofon@icrr.u-tokyo.ac.jp

Received 11 April 2003 / Accepted 28 May 2003

Abstract. The injection rate of suprathermal protons into the diffusive shock acceleration process should vary strongly over the surface of supernova remnant shocks. These variations and the absolute value of the injection rate are investigated. In the simplest case, like for SN 1006, the shock can be approximated as spherical in a uniform large-scale magnetic field. The injection rate depends strongly on the shock obliquity and diminishes as the angle between the ambient field and the shock normal increases. Therefore efficient particle injection, which leads to conversion of a significant fraction of the kinetic energy at a shock surface element, arises only in relatively small regions near the "poles", reducing the overall CR production. The sizes of these regions depend strongly on the random background field and the Alfvén wave turbulence generated due to the CR streaming instability. For the cases of SN 1006 and Tycho's SNR they correspond to about 20, and for Cas A to between 10 and 20 percent of the entire shock surface. In a first approximation, the CR production rate, calculated under the assumption of spherical symmetry, has therefore to be renormalized by this factor, while the shock as such remains roughly spherical.

Key words. ISM: supernova remnants – shock waves – acceleration of particles – ISM: cosmic rays – ISM: magnetic fields

1. Introduction

The time-dependent nonlinear kinetic theory of cosmic ray (CR) acceleration in supernova remnants (SNRs) of Berezhko et al. (1996) and Berezhko & Völk (1997, 2000), applied to the remnant of SN 1006, Tycho's supernova, and Cas A (Berezhko et al. 2002; Völk et al. 2002; Berezhko et al. 2003a), has demonstrated that the existing data are consistent with very efficient acceleration of CR nuclei at the SN shock wave, converting a significant fraction of the initial SNR energy content into CR energy. This energy is distributed between energetic protons and electrons in a proportion similar to that of the Galactic CRs.

Recent Chandra observations (Bamba et al. 2003) found the fine structure of the outer shock in SN 1006 to be characterized by extremely small spatial scales of the X-ray synchrotron emission. These structures agree very well with the above predictions and provide direct evidence for the efficient acceleration of nuclear CRs in this object (Berezhko et al. 2003b).

At the same time an essential physical factor which strongly influences the final CR acceleration efficiency is contained in our theory as a free parameter. This is the ion injection rate, i.e. the number of suprathermal protons injected into the acceleration process per unit area and unit time. It is described by a dimensionless injection parameter η that is a fixed small fraction of the interstellar medium (ISM) particles entering the shock front. Assuming spherical symmetry, this injection implies a source term $Q = Q_s\delta(r - R_s)$ due to (mono-energetic) injection at the subshock in the diffusive transport equation for the nuclear CR distribution function $f(r, p, t)$

$$\frac{\partial f}{\partial t} = \nabla(\kappa\nabla f) - \boldsymbol{w}_c\nabla f + \frac{\nabla \boldsymbol{w}_c}{3} p\frac{\partial f}{\partial p} + Q, \quad (1)$$

where Q_s is written in the form

$$Q_s = \frac{N_{inj}u_1}{4\pi p_{inj}^2}\delta(p - p_{inj}), \quad (2)$$

with $N_{inj} = \eta N_1$ and p_{inj} denoting the number of injected suprathermal particles from each unit volume intersecting the shock front and the momentum of the injected particles, respectively. Here r, t and p denote the radial coordinate, the time, and particle momentum, respectively; κ is the CR diffusion coefficient; w_c is the radial velocity of the scattering centers, $u = V_s - w$ is the flow velocity relative to the subshock at $r = R_s$, $V_s = dR_s/dt$ is the subshock velocity, $N = \rho/m$ is the proton number density, and m denotes the particle (proton) mass. The subscripts 1(2) correspond to the upstream (downstream) region.

Send offprint requests to: H. J. Völk,
e-mail: heinrich.voelk@mpi-hd.mpg.de

According to nonlinear acceleration theory, the overall shock transition consists of a thin subshock whose thickness is of the order of the gyro radius of thermal ions heated in the shock compression, and a CR precursor whose much greater spatial extent corresponds to a mean diffusion scale of the accelerated particles. Ion injection is thought to occur at the subshock. When in the following we losely refer to "the shock" in the context of injection, then we always mean the subshock.

Unfortunately there is no complete selfconsistent theory of a collisionless shock transition to the extent that it can predict the value of the injection rate and its dependence on the shock parameters for all directions of the shock normal relative to the external magnetic field vector. For the case of a purely parallel shock (where the shock normal is parallel to the external magnetic field) hybrid simulations predict quite a high ion injection rate (e.g. Scholer et al. 1992; Bennett & Ellison 1995) which corresponds to a value $\eta \sim 10^{-2}$ of our injection parameter. Such a high injection is consistent with analytical theory (Malkov & Völk 1995, 1998; Malkov 1998) and confirmed by measurements near the Earth's bow shock (Trattner & Scholer 1994).

We note however that in our spherically symmetric model these results can only be used with some important modifications. In reality we deal with the evolution of the large-scale SN shock which expands into the ISM and its magnetic field. For example in the case of SN 1006 at the current evolutionary phase the shock has a size of several parsecs. On such a scale the unshocked interstellar magnetic field can be considered as uniform since its random component is characterized by a much larger main scale of about 100 pc. Then our spherical shock is quasi-parallel in the polar regions and quasi-perpendicular in the equatorial region. The leakage of suprathermal particles from the downstream region back upstream is to leading order dependent upon the shock obliqueness which is described by the angle between the ambient magnetic field direction and the shock normal. It is most efficient for a purely parallel subshock and becomes progressively less efficient when the shock is more and more oblique (Ellison et al. 1995; Malkov & Völk 1995). Applied to a spherical shock in the uniform external magnetic field it would mean that only relatively small regions near the poles allow a sufficiently high ion injection rate which ultimately leads to the transformation of a significant part (more than a few percent) of the shock energy into CR energy, whereas the main part of the shock is an inefficient CR accelerator (Völk 2001). In this case also the field amplification due to the CR streaming instability (Völk 1984, and in particular Lucek & Bell 2000; Bell & Lucek 2001) occurs only near the poles, strongly amplifying the synchrotron emissivity there. Such a picture is consistent with the observed morphology of SN 1006: the most intense synchrotron radiation comes from two spots (Koyama et al. 1995; Allen et al. 2001), which we associate with the polar regions.

This very simple picture probably holds only for "ideal" cases like SN 1006 which lies far above the Galactic plane in a very low density and apparently quite uniform environment. For other objects, presumably already for Tycho's SNR, and certainly for all core collapse SNRs, the situation is more complex. Yet the physical arguments which we shall use should apply to all of them with appropriate modifications.

In this paper we quantitatively consider the systematic variation of the ion injection rate across the SN shock surface in a simple approximation, taking the structure of the ambient magnetic field into account. For SN explosions into a circumstellar medium that is not substantially modified by the mass loss from the progenitor star (i.e. SNe Type Ia, and core collapse SNe whose progenitor stars have zero age main sequence masses below about 15 $M_\odot$), we shall demonstrate that the size of those shock regions, where efficient injection leading to efficient CR acceleration is expected to take place, depends strongly on the random background field and the Alfvén wave turbulence generated by the CR streaming instability. For the case of SN 1006 this corresponds to about 20% of the entire shock surface, consistent with the observations. A similar result is obtained for Tycho's SNR. For the extreme case of Cas A, the final phases of stellar evolution – the red supergiant (RSG) and the subsequent Wolf-Rayet phase – have produced a complex circumstellar pattern of the magnetic field. It is characterized by an essentially azimuthal mean field of stellar origin with superposed MHD waves, and strongly modified on large scales by instabilities due to the radial forces which have their origin in the late appearance of a high-luminosity Wolf-Rayet phase. An approximate calculation gives the result that only on a fraction of about 10 to 20% of the shock surface ion acceleration proceeds efficiently.

Electron injection is a rather different problem and our understanding is much poorer. In many ways, however, electron injection can be discussed seperately. We will briefly adress it in Sect. 6. While it is an essential ingredient for the synchrotron and the inverse Compton emission, to lowest order it neither affects the ion acceleration nor the overall SNR dynamics.

2. Spherical shock in a uniform external magnetic field

Figure 1 schematically illustrates a spherical shock in a uniform ambient magnetic field $\boldsymbol{B}$. In the simplest MHD approximation, the magnetic field structure in the downstream region is determined by the compression of the component perpendicular to the shock normal and is described by the relations:

$$B_{2\parallel} = B_{1\parallel}, \qquad B_{2\perp} = \sigma B_{1\perp}, \tag{3}$$

where σ is the shock compression ratio, $B_\parallel = B\cos\theta$, $B_\perp = B\sin\theta$.

Since all the scales that characterize the motion of thermal particles are very much smaller than the shock size, a plane wave approach can be used for their description. Figure 2 illustrates the magnetic field structure near the subshock front. The cold upstream plasma is advected with speed $u_1 = V_s$ towards the shock front, is compressed and heated, and flows with speed $u_2 = u_1/\sigma$ into the downstream region. Very fast particles from the thermalised downstream population, whose velocity exceeds some critical value $v_{\rm inj}$ and which move towards the shock front, are able to overtake it and to penetrate into the upstream region. Since the particle mobility increases

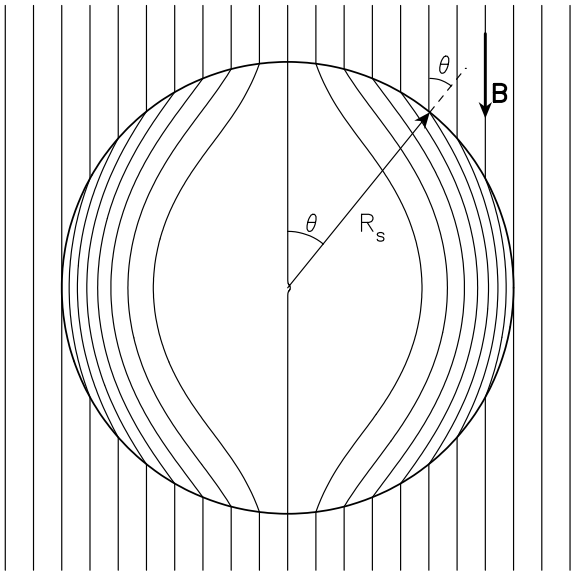

Fig. 1. Schematic form of the interstellar magnetic field lines, modified by a spherically expanding shock (*thick circle*).

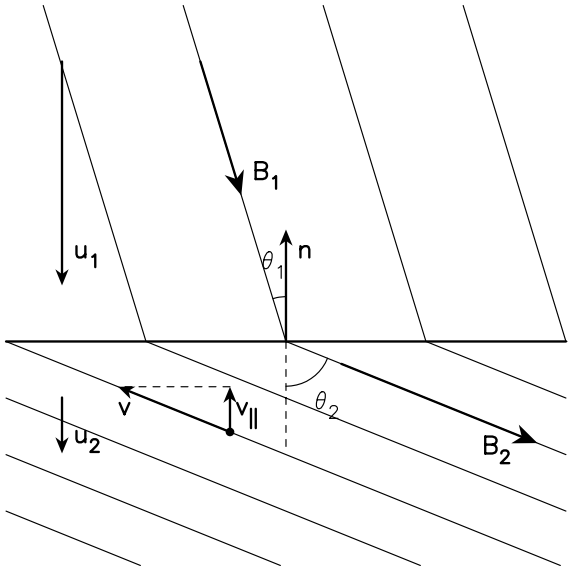

Fig. 2. Schematic picture of the local magnetic field and the flow structure near the shock front.

with their speed v, these particles can be considered as diffusive and they gain energy in their random walk across the shock. Asymptotically, for velocities $v \gg v_{\rm inj}$ (e.g. Malkov & Völk 1995), their pitch angle distribution approximates an isotropic distribution.

The number of these injected particles is determined by the structure of the subshock transition (Malkov 1998; see Fig. 1 from Malkov & Völk 1998). The most important physical parameter which determines this number is the particle velocity parallel to the shock normal $v_\parallel$: all particles which have $v_\parallel > v_{\rm inj}$ are considered as injected. It is assumed that the mean free path of the particles which have a speed higher than the threshold $v_{\rm inj}$ exceeds the thickness of the subshock.

Assuming the injected particles to come from the tail of a Maxwellian distribution we can write

$$\eta_\parallel = \exp\left(-v_{\rm inj}^2/v_{\rm T2}^2\right), \tag{4}$$

where $v_{\rm T2}$ is the mean thermal speed of the downstream particle population. As mentioned above, numerical simulations of parallel collisionless shocks give an expected injection rate $\eta_\parallel = \eta(\theta_1 = 0) \approx 10^{-2}$ (e.g. Scholer et al. 1992; Bennett & Ellison 1995), that leads to the value $v_{\rm inj} = 2v_{\rm T2}$ of the injection velocity.

We assume that the suprathermal particles are strongly magnetized. Therefore, for any magnetic field direction, the condition that selects injected particles is $v_\parallel > v_{\rm inj}$. Since $v_\parallel = v\cos\theta_2$ this means that only those particles are injected which move towards the shock front and have speed $v > v_{\rm inj}/\cos\theta_2$. Taking into account the relation

$$\cos^2\theta_2 = \left(1 + \sigma^2\tan^2\theta_1\right)^{-1} \tag{5}$$

one finds

$$\eta(\theta_1) = \eta_\parallel^{1+\sigma^2\tan^2\theta_1}. \tag{6}$$

According to this relation the injection rate goes down quickly with increasing upstream angle θ_1, as illustrated by the curve which corresponds to $\delta B = 0$ in Fig. 3: for $\theta_1 = 10^\circ$ the injection rate is one order of magnitude, and for $\theta_1 = 20^\circ$ it is four orders of magnitude smaller than for $\theta_1 = 0^\circ$.

This simple relation (6) is a direct consequence of our assumption that all particles are able to propagate only along the magnetic field lines. In reality they will to some extent also undergo cross field motion, either due to drift motions or due to cross field diffusion. On the other hand this cross field motion can be substantial only for a relatively high random field component. As shown below, a high-amplitude random field allows efficient particle injection also within our simplified approach.

It is important to note that there exists a so-called critical injection rate from the solution of the nonlinear kinetic Eq. (1), coupled with the hydrodynamics of the thermal gas. The value of this critical injection rate is approximately determined by the expression (Berezhko & Ellison 1999)

$$\eta_{\rm crit} = 10^{-1}\frac{V_{\rm s}}{c}\left(\frac{p_{\rm max}}{mc}\right)^{-1/4}, \tag{7}$$

where c is the speed of light and $p_{\rm max}$ is the maximum momentum of the accelerated CRs. It divides the region $\eta > \eta_{\rm crit}$ of the efficient CR acceleration, when a significant fraction of the shock energy goes into CR energy, from the region $\eta < \eta_{\rm crit}$ of inefficient CR acceleration. For $V_{\rm s} = 3000\ {\rm km\,s^{-1}}$ and $p_{\rm max} \sim 10^5\ mc$ the critical injection rate is $\eta_{\rm crit} = 6 \times 10^{-5}$. This means that in the case of SN 1006, if we do not take into account the hitherto disregarded random magnetic field component, efficient CR production is expected to occur only within two polar regions with $\theta_1 < \theta_{\rm max} = 14^\circ$. This angular width is considerably smaller than the one observed (e.g. Koyama et al. 1995; Allen et al. 2001).

3. Magnetic field fluctuations

The existence of a random magnetic field component $\delta\boldsymbol{B}$ on scales large compared to the thickness of the subshock can

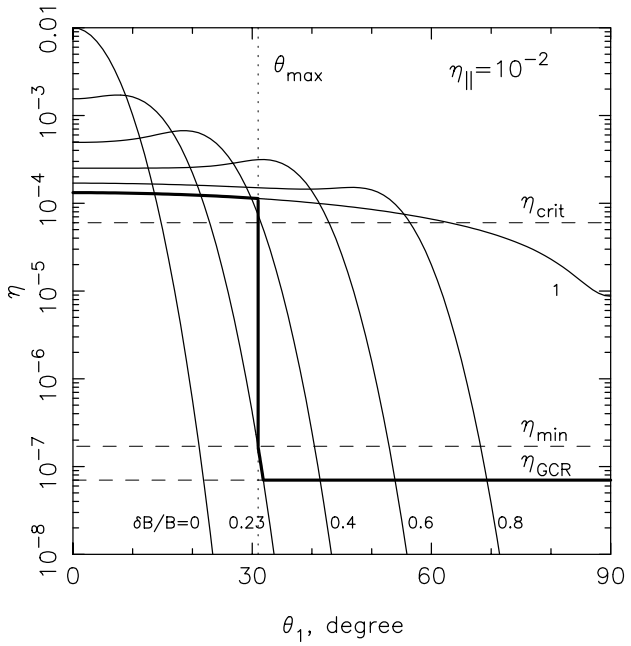

Fig. 3. The injection rate η as a function of the upstream angle θ_1 between the ambient magnetic field and the shock normal, for different amplitudes $\delta B/B$ of the upstream random field (*solid lines*), given that $\eta_{||} = 10^{-2}$, for the current parameters of SN 1006. *Dashed lines* represent the critical injection rate η_{crit}, the minimal injection rate η_{min} required to provide significant random field amplification, and the injection rate η_{GCR} which is equivalent to GCR reacceleration. The *thick solid line* represents the expected current injection rate; the vertical *dotted line* indicates the corresponding angular region of efficient injection/acceleration.

change the value of the injection rate. To study this effect we assume that the ambient field

$$\boldsymbol{B'}_1 = \boldsymbol{B}_1 + \delta\boldsymbol{B} \tag{8}$$

consists of two components, the uniform field $\boldsymbol{B}_1$, and a superimposed, isotropically distributed random component $\delta\boldsymbol{B}$. If the spatial scale of the random component is much smaller than the shock size R_s, one can find the mean injection rate by averaging over the directions of the random field:

$$\eta = \frac{1}{4\pi}\int \mathrm{d}\Omega_{\delta\boldsymbol{B}} \eta_{||}^{1+\sigma^2\tan^2\theta'_1}. \tag{9}$$

Here θ'_1 is the angle between $\boldsymbol{B'}_1$ and the shock normal direction $\boldsymbol{n}$, in analogy to Fig. 2. The averaging procedure either corresponds to an average over a time interval which is short compared with the shock age and large compared with the relevant periods of resonantly scattering field fluctuations for injected particles, or to a spatial average within the shock region whose size is small compared with the shock size and large compared with the scales of the relevant scattering field fluctuations.

The averaged injection rate as a function of angle θ_1 for different random field amplitudes $\delta B/B$ is shown in Fig. 3. At small angles θ_1, where the shock is almost purely parallel, field fluctuations make it more oblique for some fraction of the time. The opposite is true for large θ_1. Therefore, as one can see in Fig. 3, the existence of the random field component leads to a decrease of the injection rate at small angles and to an increase at large angles θ_1, so that at the highest values of the turbulent field $\delta B/B = 1$, compared to an ideal parallel shock, the injection rate is reduced by almost two orders of magnitude to a value $\eta(\theta_1) \approx 10^{-4}$ which becomes almost uniform across an angular range $\theta_1 \leq 63°$.

4. Selfconsistent turbulent field

The random magnetic field component $\delta\boldsymbol{B}$ can be created selfconsistently by the CR streaming instability in the upstream region (Bell 1978; Blandford & Ostriker 1978). The expected amplitude of the Alfvén waves excited due to the CR streaming instability is determined by the expression (McKenzie & Völk 1982; Bell & Lucek 2001)

$$\left(\frac{\delta B}{B}\right)^2 = \frac{V_s}{c_a}\frac{P_c}{\rho V_s^2}, \tag{10}$$

where c_a is the Alfvén speed,

$$P_c = \frac{4\pi}{3}\int_{p_{inj}}^{p_{max}} \mathrm{d}p\, pv f(p) \tag{11}$$

is the CR pressure at the shock front, p_{inj} and p_{max} are the injection and maximum CR momenta, respectively, and f is the solution of Eq. (1) in which the injection rate appears as a given source term. Since we consider effects which can increase an initially very low injection rate, the shock modification by the CR pressure is neglected and a plane wave approximation is used. Within this approach the CR distribution function at the shock front can be written in the form (e.g. Berezhko et al. 1996)

$$f = \frac{qN_{inj}}{4\pi p_{inj}^3}\left(\frac{p}{p_{inj}}\right)^{-q}, \tag{12}$$

where $q = 3u_1/(u_1 - u_2)$. Taking into account that in the case of a strong unmodified shock ($q = 4$) the appropriate value of the injected particle speed is $v_{inj} \approx 2V_s$, and that relativistic particles with $mc < p < p_{max}$ provide the main contribution to the CR pressure, we can write

$$\left(\frac{\delta B}{B}\right)^2 = \frac{8c\eta}{3c_a}\ln\frac{p_{max}}{mc}. \tag{13}$$

The quantity $\ln(p_{max}/mc)$ depends at most logarithmically on $(\delta B/B)^2$. As a consequence it can be seen from this relation that, once the selfconsistent Alfvén wave field δB exceeds the background ISM fluctuation field δB_0 (see Sect. 7), then any initially low injection rate leads to the growth of the random magnetic field in the upstream region which in turn leads to an increase of the injection rate (see Fig. 3). Equating $(\delta B/B)^2$ to the background level $(\delta B/B)_0^2$ we can find the minimal initial injection rate

$$\eta_{min} = \frac{3c_a}{8c\ln(p_{max}/mc)}\left(\frac{\delta B}{B}\right)_0^2. \tag{14}$$

On account of the Alfvén wave generation by the CR streaming instability the expected high efficiency injection region is bounded by the polar angle $\theta_{\rm max}$ determined from the relation

$$\eta(\delta B, \theta_{\rm max}) = \eta_{\rm min}, \tag{15}$$

where $\eta(\delta B, \theta_1)$ is the function shown in Fig. 3 for a given random field amplitude δB. Within the region $\theta_1 < \theta_{\rm max}$ the initial injection rate is high enough so that accelerated particles are able to increase the level of the turbulence level which in turn increases the injection rate. This selfconsistent nonlinear amplification also increases the mean magnetic field strength to an effective mean field B whose difference to the actual field defines an effective δB (Lucek & Bell 2000). The process can be assumed to end when the amplitudes of the Alfvén waves become so high that $\delta B \sim B$ for the effective quantities and their further growth is prevented by strong nonlinear dissipation processes. Identifying therefore $(\delta B/B)$ in Fig. 3 for $\theta_1 < \theta_{\rm max}$ with the ratio of the effective quantities, the expected selfconsistent injection rate corresponds to the curve $\eta(\delta B = B, \theta_1)$.

The amplification of the field to an effective field large compared to the external field B_1 is an important aspect of CR production, since it determines the value of the maximum CR energy. At the same time, this strongly modified upstream field remains completely randomized. Therefore we assert that the injection rate within the region $\theta_1 < \theta_{\rm max}$ is not sensitive to the specific value of the upstream magnetic field B_1.

5. Background cosmic ray acceleration

Suprathermal particle leakage from downstream is not the only mechanism that supplies particles to the diffusive shock acceleration process. Galactic cosmic rays (GCRs) are also subject to further acceleration, sometimes also called re-acceleration. We assume that the majority of GCRs participating in this reacceleration have a momentum $p \simeq mc$ and therefore their number density can be estimated as

$$N_{\rm GCR} = e_{\rm GCR} / \left(mc^2\right), \tag{16}$$

where $e_{\rm GCR} \approx 0.6$ eV/cm^3 is the GCR energy density. Comparing the number of CRs with momenta $p \geq mc$, produced in shock acceleration at a given injection rate η, with $N_{\rm GCR}$, we can define a minimal injection rate of suprathermal protons

$$\eta_{\rm GCR} = \frac{cN_{\rm GCR}}{8V_{\rm s}N_{\rm H}}, \tag{17}$$

below which GCR re-acceleration becomes more efficient than acceleration of suprathermal particles.

It can be seen from the above expression that the role of GCR re-acceleration increases with decreasing shock speed and/or ISM gas number density. Therefore it can become significant in the diluted ISM during late SNR evolutionary phases, or for SN explosions in the hot and low density ISM of elliptical galaxies (Dorfi & Völk 1996).

Since re-acceleration of GCRs is almost independent of the polar angle θ_1 (Drury 1983), efficient CR production will occur practically over the whole SN shock surface, if $\eta_{\rm GCR}$ exceeds the critical injection rate $\eta_{\rm crit}$.

In the case $\eta_{\rm GCR} < \eta_{\rm crit}$ the role of GCRs can be still significant if $\eta_{\rm GCR} > \eta_{\rm min}$. Since at large angles θ_1 GCR reacceleration dominates over the suprathermal particle acceleration, Alfvén wave generation due to reaccelerated GCRs is also higher: they produce in the upstream region an Alfvén wave field

$$\left(\frac{\delta B}{B}\right)^2 = \frac{\eta_{\rm GCR}}{\eta_{\rm min}} \left(\frac{\delta B}{B}\right)_0^2. \tag{18}$$

Therefore, efficient injection in this case occurs within the angular range $\theta_1 < \theta_{\rm max}$ where $\theta_{\rm max}$ is determined from the relation $\eta(\delta B, \theta_{\rm max}) = \eta_{\rm GCR}$, with δB from expression (18).

6. Electron injection

The injection of electrons is a different problem and is much less well understood physically. We shall give here a very brief discussion in order to connect synchrotron and, possibly, inverse Compton emission to the dynamics and radiation properties of accelerated nuclei in SNRs.

Suprathermal electrons from the hot downstream region cannot resonantly scatter on the MHD waves produced by the escaping ions, and other wave types have to be investigated (Levinson 1996). On the other hand, in more or less perpendicular shocks, reflection of part of the incoming ion population back into the upstream plasma is possible, exciting electrostatic waves there in which electrons can be energized. This energization can certainly inject these electrons into the diffusive shock acceleration process if the electrons reach GeV energies from which point on they accelerate like relativistic ions of comparable kinetic energies. Models of this kind have been investigated after the pioneering study of Galeev (1984) by Galeev et al. (1995), McClements et al. (1997) and Dieckmann et al. (2000). This suggests that, in contrast to ions, electrons may be even best injected at rather perpendicular shocks. Since the spatial and temporal scales of this initial electron energization are very short, this argument can presumably be applied locally to any part of the shock surface where the shock normal is highly oblique to the local instantaneous magnetic field. Since furthermore in the quasi-parallel shock regions the energetically dominant accelerating ions create large amplitude MHD waves, there may thus be *parasitic* electron injection and acceleration also in these regions. Altogether, electron injection might therefore occur more or less everywhere over the SNR shock surface. Whether this can hold also for subsequent acceleration to the highest energies, is a quite different matter, and less than clear.

Let us nevertheless assume that electrons are uniformly injected and even accelerated across the SNR shock. The resulting synchrotron emission is $\propto B^{(q-1)/2}$ and will therefore still occur predominantly in the polar regions with their strong turbulent field amplification, despite the average field compression in the equatorial region (see next section). The Inverse Compton gamma-ray emission may, however, be fairly uniform over the SNR surface.

7. Results and discussion

As a representative case, we first apply the above formalism to SN 1006. For the relevant SN 1006 parameters $V_s = 3200\,\mathrm{km\,s^{-1}}$, and $N_H = 0.1\,\mathrm{cm^{-3}}$ we have $\eta_{GCR} = 7 \times 10^{-8}$.

Since the interstellar random magnetic field is distributed over a wide range of scales λ, only part of this spectrum with scales $\lambda < \lambda_{max}$ has to be considered as the small scale field. The upper scale can be taken as the diffusive length of the highest energy CRs accelerated, i.e. $\lambda_{max} = l(p_{max})$. According to our numerical results (Berezhko et al. 2002), for the current evolutionary phase of SN 1006, $p_{max} = 4 \times 10^5\ mc$ and $l(p_{max}) = 0.08\ R_s$. Assuming that the energy density per unit logarithmic scale interval of the background ISM turbulent field as function of the spatial length λ increases according to the Kolmogorov law

$$E_w(\lambda) = \left(\frac{\lambda}{L_0}\right)^{2/3} \left(\frac{B_0}{8\pi}\right)^2 , \tag{19}$$

we find that for scales smaller than $\lambda_{max} = 0.08\,R_s$ it has a value $(\delta B/B)_0^2 = \int_0^{\lambda_{max}} \mathrm{d}\ln\lambda E_w/(B_0^2/8\pi) = 5.3 \times 10^{-2}$, or $(\delta B/B)_0 = 0.23$, taking into account that the main scale is $L_0 = 100$ pc. According to Eq. (14), for a typical ISM magnetic field $B_0 = 3\,\mu$G and a moderate maximum CR momentum $p_{max} = 10^3 mc$, we have in this case $\eta_{min} = 1.7 \times 10^{-7}$. Since $\eta_{GCR} < \eta_{min}$, GCR re-acceleration does not play an important role in this case.

As one can see from Fig. 3, the line $\eta(\theta_1)$ which corresponds to $\delta B/B = 0.23$ intersects the minimal level $\eta_{min} = 1.7 \times 10^{-7}$ at $\theta_{max} = 31°$. This means that an initial injection level represented by this curve $\eta(\theta_1)$ leads within the whole region $\theta_1 < 31°$ to progressive growth of Alfvén waves, which in turn leads to a corresponding increase of the injection rate. As argued above, this positive backreaction drives the field amplification to the point $\delta B/B \sim 1$. Therefore the expected injection rate $\eta \approx 10^{-4}$ at $\theta_1 < 31°$ corresponds to the curve $\eta(\delta B = B, \theta_1)$. Since $\eta > \eta_{crit}$, efficient CR production will occur in this angular region. For $\theta_1 > \theta_{max}$ the expected injection rate $\eta(\theta_1)$ goes along the curve $\eta(\delta B/B = 0.23, \theta_1)$ and then along $\eta = \eta_{GCR}$. For all $\theta_1 > \theta_{max}$ the expected injection rate is lower than the critical rate.

Then we have the situation where a sharp boundary $\theta_1 = \theta_{max}$ separates the regions of efficient and inefficient CR injection/acceleration. One has to expect that in reality this boundary is smoothed as a result of some additional physical process. Possibly the most important factor is the cross-field diffusion of CRs. Due to the high level of selfconsistent turbulence within the region $\theta_1 < \theta_{max}$, CR diffusion is almost isotropic. High energy CRs with $p > mc$ will therefore be able to penetrate diffusively through the boundary $\theta_1 = \theta_{max}$ in the upstream region. They can also be accelerated in a finite region $\theta_1 > \theta_{max}$. An approximate CR diffusion length across the regular magnetic field in the upstream region is their parallel diffusion length $l(p_{max})$. It corresponds to the angle interval $\Delta\theta_1 = (l/R_s)$ rad $\approx 5°$. This means that the smoothed region of efficient CR acceleration extends up to $\theta'_{max} = \theta_{max} + \Delta\theta \approx 36°$. Therefore efficient particle injection/acceleration is expected to occur within a bipolar region of about 20% of the shock surface. Its size corresponds rather well to that of the observed bright X-ray synchrotron emission regions of SN 1006 (e.g. Allen et al. 2001)[1].

7.1. Renormalization

According to the above estimate, a substantial part of the shock still efficiently injects and accelerates CRs. In addition, the overall conservation equations ensure an approximately spherical character of the overall dynamics. Therefore, we assume the spherically symmetric approach for the nonlinear particle acceleration process to be approximately valid in those shock regions where injection is efficient. To take this injection fraction

$$f_{re} = 1 - \cos\theta'_{max} \tag{20}$$

into account, we need then to introduce a *renormalization* factor for the overall nuclear CR acceleration efficiency, and for all the effects which it produces in the SNR. According to the above estimate its value in the case of SN 1006 is $f_{re} \approx 0.2$.

7.2. Synchrotron emission

The amplification of the magnetic field in the region of efficient acceleration leads to an effective downstream field strength of $120\,\mu$G strength that exceeds the mean interstellar field of about $3\,\mu$G by a factor of 40, according to the comparison of the synchrotron measurements for SN 1006 with the theoretical model (Berezhko et al. 2002). Outside the ion injection region, in the "equatorial" region, there is by definition no shock modification and the interstellar field is at most compressed by a factor of 4, corresponding to a strong adiabatic shock in the thermal plasma. In fact, the field compression factor is on average smaller than 4 because the shock is truly perpendicular only on the equator itself. Therefore the enhancement of the local synchrotron emissivity in the polar regions relative to the equatorial region exceeds $10^{1.5} \approx 32$ for the hard particle spectrum $\propto p^{-2}$. The spatially integrated emissivities must be adjusted by the ratio $f_{re}/(1 - f_{re}) = 1/4$ of the polar to the equatorial areas. Therefore the global excess emissivity of the polar regions is expected to be 8 times larger than the equatorial emissivity on account of the higher magnetic field. As a consequence we expect the polar regions to dominate also the synchrotron radiation, in contrast to the arguments of Ratkiewicz et al. (1994) who assumed that the uniform ISM field is merely MHD-compressed by the spherical shock, which would then obviously lead to maximum emissivity in the equatorial region.

7.3. The case of Tycho's Supernova

Until now we have given numbers that refer to SN 1006. Also the discussion of morphological effects was done for this ideal case. Even though Tycho's SN was also of type Ia, its present

[1] We shall not go into speculations here whether the nonlinear wave amplification process can spread into SNR surface regions where the shock is practically perpendicular, so to say by itself. While such a scenario can not be excluded theoretically at this time, we believe that it is more fruitful to ask whether the observations give any hint in this direction. From present knowledge they do not.

X-ray emission is dominated by line radiation, and not by nonthermal emission, like SN 1006. In addition, the ambient interstellar medium around Tycho appears to be unexpectedly nonuniform, cf. Reynoso et al. (1997). As a consequence, it is not clear whether we can expect a nonthermal X-ray morphology as simple as that of SN 1006. Nevertheless, the magnetic field topology is analogous and therefore we shall calculate the renormalization factor in an analogous form.

With a present radius $R_s \approx 2.7$ pc and a mean ambient density $N_H = 0.5$ cm^{-3}, Tycho is smaller than SN 1006 and the ambient density is considerably higher, whereas the present shock velocity $V_s = 3100$ km s^{-1} is about the same. This gives $\eta_{min} = 2.4 \times 10^{-6}(\delta B/B)_0^2$. Similarly, we have $(\delta B/B)_0^2 = 3/2(\lambda_{max}/L_0)^{2/3}$ with $\lambda_{max} = 0.27$ pc. Taking the turbulent main scale L_0 proportional to the critical SNR radius at cooling which in turn is proportional to $N_H^{-1/3}$, we have $L_0 = 58.5$ pc for Tycho, if $L_0 = 100$ pc for SN 1006. This gives $(\delta B/B)_0 = 0.2$, and finally $f_{re} = 0.18$ for Tycho, roughly similar to the value for SN 1006, as used in Völk et al. (2002).

7.4. Late phases

Since the energy density of the random component of the background field $(\delta B/B)_0^2 \propto R_s^{2/3}$ increases during the SNR evolution, the size of the region of efficient injection becomes progressively larger as well. In the extreme case of a shock with size $R_s \sim 100$ pc – provided it is still strong enough – efficient injection/acceleration occurs across the entire shock surface due to the completely randomized background field on the scale R_s. This situation makes the contribution of the late SNR evolutionary phases more important, and therefore the resultant CR energy spectrum produced in such SNRs is expected to be steeper compared with the model prediction in spherical symmetry.

According to expression (7) the critical injection rate goes down proportionally to the shock speed V_s, whereas the injection rate (17) due to GCRs is inversely proportional to V_s. Therefore the significance of GCR reacceleration in the sense of an injection mechanism progressively increases during SNR evolution. When the shock speed drops to the value $V_s \approx 35/\sqrt{N_H/(1\ \mathrm{cm}^{-3})}$ km s^{-1}, η_{GCR} exceeds η_{crit} and then the GCRs alone lead to efficient CR acceleration across the whole shock surface. Since the GCR chemical composition differs from the ISM composition, GCR re-acceleration can play a role in determining the resultant chemical composition.

7.5. Renormalization factor for Cas A

A much more complicated situation arises in SNRs where the circumstellar medium is strongly influenced by the wind from the progenitor star. Cas A is a prominent example. According to the analysis of the thermal X-ray emission, and consistent with the observed overall dynamics of Cas A, the supernova shock expands into an inhomogeneous circumstellar medium strongly modified by the intense wind of the progenitor star (Borkowski et al. 1996). It consists of a tenuous inner bubble, created by the Wolf-Rayet (WR) wind, a dense shell of swept-up, slow red supergiant wind (RSG) material, and a subsequent free RSG wind. The ambient magnetic field structure is not well known in this case. Therefore it is not possible to perform an equally definite analysis of the expected injection rate as for type Ia SNe. As we shall demonstrate below, quite a reasonable estimate can nevertheless be obtained.

Due to the progenitor star's rotation, the mean large-scale magnetic field is expected to be almost purely tangential to the shock surface in the wind material. At the same time, as shown in numerical simulations (Garcia-Segura et al. 1996), the interaction of the fast WR with the slow, massive RSG wind and the shell formation is accompanied by a long-wavelength instability. We assume that this instability is able to strongly randomize the preexisting field in the shell, and to possibly even amplify it. Therefore the ambient circumstellar magnetic field seen by the SNR shock in the shell should consist of three components

$$\boldsymbol{B}_1 = \langle \boldsymbol{B} \rangle + \delta \boldsymbol{B}_l + \delta \boldsymbol{B}_s, \tag{21}$$

a mean field $\langle \boldsymbol{B} \rangle$ which is practically everywhere tangential to the shock surface, a large-scale random component ($\delta \boldsymbol{B}_l$), and a small-scale random component ($\delta \boldsymbol{B}_s$). The small-scale field component consists of the copious amount of MHD waves, essentially Alfvén waves, emitted by the central RSG, and is expected to follow a nonlinear cascade towards short scales, taken here to be of the Kolmogorov type.

We shall assume an analogous magnetic field structure in the outer free RSG wind region (Berezhko et al. 2003a). The relevant instability there is that of radiation pressure-driven winds (Lucy & White 1980; for a more recent discussion, see Lucy 1984) which we consider here in terms of the dynamical effect of the intense WR star radiation field on the free RSG wind.

During the SNR shock propagation through the RSG wind material, the variation of the random magnetic field component will lead in both phases – compressed shell and free RSG wind – to a number of irregular regions (spots) on the shock surface where the shock is quasi-parallel, whereas the main fraction of the shock is quasi-perpendicular[2].

The fraction of the shock surface f_{re} where the shock is quasi-parallel and where therefore efficient injection occurs, depends on the ratios of the values of the magnetic field components $\langle B \rangle$, δB_l and δB_s. In order to estimate the expected value of the renormalization factor f_{re} for given values of $\langle B \rangle$, δB_l and δB_s, we first calculate the injection rate $\eta(\theta_1)$ by performing the averaging procedure over all possible directions of the small scale random field $\boldsymbol{B}_s$ according to the expression (9), where in this case $\boldsymbol{B}_1 = \langle \boldsymbol{B} \rangle + \boldsymbol{B}_l$ and $\delta \boldsymbol{B} = \delta \boldsymbol{B}_s$. Subsequently, we can calculate the value of the solid angle $\Delta\Omega$ which includes those components of the large scale random field $\delta \boldsymbol{B}_l$ whose directions lead to efficient injection, that is $\eta(\theta_1) > \eta_{min}$. In the spirit of Fig. 3, we then assume that above η_{min} injection rises nonlinearly as a result of strong acceleration, if the typical scales of

[2] Similar regions with irregular shock normal angles relative to the magnetic field will be produced by the clumpy nature of the SN ejecta – the fast moving knots – which give the SNR shock a rather frayed appearance. For lack of better knowledge we shall lump the two effects together here into a single component δB_l.

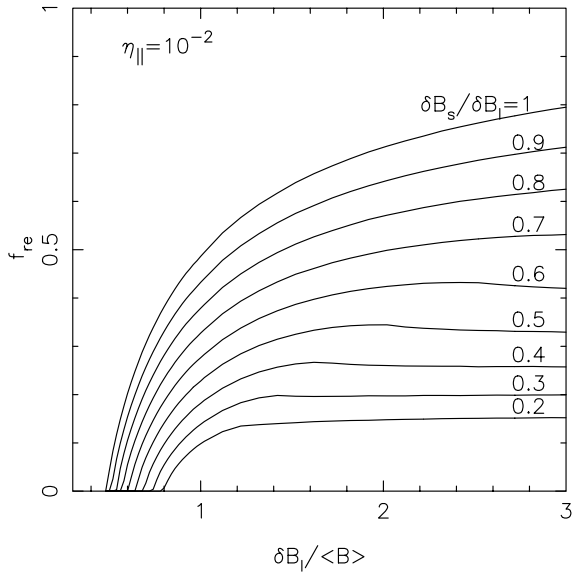

Fig. 4. The renormalization factor $f_{\rm re}$ as a function of the random large-scale magnetic field component, for different values of the small-scale field component $\delta B_{\rm s}$.

the high-injection flux tubes exceed the size $l(p_{\rm max}) \approx 0.1\,R_{\rm s}$ of the CR precursor. This is expected to be the case at least in the compressed shell of Cas A, judging from the numerical results of Garcia-Segura et al. (1996). In the outer free RSG region we have also assumed this to be true in the model of Berezhko et al. (2003a). However, it is not clear how large the radial scales of the radiation-induced instability are, even though the scales of the frayed shock due to the fast moving ejecta knots should be the same as in the shell. Therefore the efficient acceleration also in the free RSG wind remains an assumption which we shall also make here. Quantitatively, the radio and X-ray flux from the dense shell dominates the overall nonthermal emission in these wavelength regions at the present epoch (Berezhko et al. 2003a), so that the contribution from the free RSG wind is not a decisive factor in the interpretation of the gamma-ray emission from Cas A.

Since the gas number density in the shell is $N_{\rm g} = 10\ {\rm cm}^{-3}$ and the magnetic field value is about $B_0 = 200\,\mu$G, the Alfvén speed is $c_{\rm a} = 130\,{\rm km\,s}^{-1}$ which gives $\eta_{\rm min} = 1.4{\times}10^{-5}\,(\delta B/B)_0^2$, where $\delta B = \delta B_{\rm s}$ and $B = \langle B\rangle + \delta B_{\rm l}$. Because the large-scale field component $\delta \boldsymbol{B}_{\rm l}$ is randomly distributed, the value of the renormalization factor is determined by the simple expression

$$f_{\rm re} = \Delta\Omega/(4\pi). \qquad (22)$$

The value of the renormalization factor $f_{\rm re}$ as a function of $\delta B_{\rm l}/\langle B\rangle$, calculated for different ratios of small-scale to large-scale field components $\delta B_{\rm s}/\delta B_{\rm l}$, is shown in Fig. 4. One can see that for $\delta B_{\rm l} \sim \langle B\rangle$ the renormalization factor $f_{\rm re}$ has values between 0.1 and 0.2 if the small-scale random component has a relative amplitude $\delta B_{\rm s}/\delta B_{\rm l}$ between 0.2 and 0.4. Such relative amplitudes appear quite realistic.

We conclude that the value $f_{\rm re} = 0.15$, which yields a satisfactory description of all relevant properties of the emission generated in Cas A by accelerated CRs (Berezhko et al. 2003a), is indeed consistent with the expected structural properties of the circumstellar magnetic field.

8. Summary

The injection rate of suprathermal particles into the shock acceleration process depends strongly on the shock obliquity and diminishes as the angle between the ambient field and the shock normal increases. For the ideal case of a SN explosion into a uniform interstellar medium with a uniform magnetic field $\boldsymbol{B}$, efficient particle injection, leading to the conversion of a significant fraction of the kinetic energy at a shock surface element, only occurs in relatively small regions near the "poles", reducing the overall CR production. The sizes of these regions depend strongly on the random background field and on the Alfvén wave turbulence generated upstream of the shock due to the CR streaming instability.

For SN 1006 which appears to approximate this ideal case, efficient CR production is expected to arise within two polar regions, where the SN shock is quasi-parallel. The relative size of these regions depends decisively on the amplitude of the random background field component δB: it changes from a fraction of about 0.07 to one of 0.7 of the shock surface when the interstellar random field amplitude varies from $\delta B/B = 0$ to 1, respectively. It is argued that the nonlinear backreaction of wave production on the injection rate leads to a definite size of the injection fraction.

It is also argued that the actual spatially integrated nuclear gamma-ray emission from such objects can be obtained through a renormalization of the spherically symmetric result by the same factor.

For SN 1006, the calculated size of the efficient CR production regions which amounts to about 20% of the shock surface corresponds very well to the observed sizes of the bright X-ray synchrotron emission regions (e.g. Koyama et al. 1995; Allen et al. 2001). This implies a renormalization factor of 0.2.

In the case of Tycho's SNR, with its unexpectedly nonuniform ambient interstellar medium, we can not expect such a simple X-ray morphology. However, at least the topology of the field should be the same. Therefore the renormalization factor $f_{\rm re}$ has been calculated in an analogous manner. Although the relevant parameters differ from those of SN 1006, we obtain the similar value $f_{\rm re} = 0.18$.

The total size of the regions where efficient injection of suprathermal particles occurs and the relevance of GCR reacceleration are expected to increase during SNR evolution. This leads to a steepening of the resultant energy spectrum of CRs produced in SNRs compared with the spherically symmetric case.

In the case of a circumstellar medium which is strongly perturbed by the mass loss of the progenitor star, like it exists for Cas A, efficient injection presumably takes place in a number of randomly distributed portions of the shock surface with quasi-parallel magnetic field. The fraction of the shock surface covered by these spots depends on the relative strength of the mean magnetic field, which is assumed to be tangential to the shock surface, and upon the amplitude ratio of the small-scale and the large-scale scale random field components. It is larger

for lower mean field values and for higher small-scale random fields. It was demonstrated that quite reasonable magnetic field parameters are consistent with efficient injection on about 15% of the shock surface, the fraction which is required in order to reproduce the observed properties of Cas A (Berezhko et al. 2003a).

Acknowledgements. This work has been supported in part by the Russian Foundation for Basic Research (grants 03-02-16325, 99-02-16325). EGB and LTK acknowledge the hospitality of the Max-Planck-Institut für Kernphysik, where part of this work was carried out. LTK also acknowledges the receipt of JSPS Research Fellowship.

References

Allen, G. E., Petre, R., & Gotthelf, E. V. 2001, ApJ, 558, 739
Bamba, A., Yamazaki, R., Ueno, M., & Koyama, K. 2003, ApJ, 589, 827
Bell, A. R. 1978, MNRAS, 182, 147
Bell, A. R., & Lucek, S. G. 2001, MNRAS, 327, 433
Bennet, L., & Ellison, D. C. 1995, JGR, 100, 3439
Berezhko, E. G., Elshin, V. K., & Ksenofontov, L. T. 1996, JETP, 82, 1
Berezhko, E. G., & Völk, H. J. 1997, Astropart. Phys., 7, 183
Berezhko, E. G., & Ellison, D. C. 1999, ApJ, 526, 385
Berezhko, E. G., & Völk, H. J. 2000, A&A, 357, 183
Berezhko, E. G., Ksenofontov, L. T., & Völk, H. J. 2002, A&A, 395, 943
Berezhko, E. G., Pühlhofer, G., & Völk, H. J. 2003a, A&A, 400, 971
Berezhko, E. G., Ksenofontov, L. T., & Völk, H. J. 2003b, A&AL., submitted
Blandford, R. D., & Ostriker, J. P. 1978, ApJ, 22, L29
Borkowski, K. J., Szymkowiak, A. E., Blondin, J. M., & Sarazin, C. L. 1996, ApJ, 466, 866
Dieckmann, M. E., McClements, K. G., Chapman, S. C., et al. 2000, A&A, 356, 377
Dorfi, E. A., & Völk, H. J. 1996, A&A, 307, 715
Drury, L. O'C. 1983, Rep. Prog. Phys., 46, 973
Ellison, D. C., Baring, M. G., & Jones, F. C. 1995, ApJ, 453, 873
Galeev, A. A. 1984, Sov. Phys., JETP, 59, 965
Galeev, A. A., Malkov, M. A., & Völk, H. J. 1995, J. Plasma Phys., 54, 59
Garcia-Segura, G., Langer, N., & Mac Low, M.-M. 1996, A&A, 316, 133
Koyama, K., Petre, R., Gotthelf, E. V., et al. 1995, Nature, 378, 255
Levinson, A. 1996, MNRAS, 278, 1018
Lucek, S. G., & Bell, A. R. 2000, MNRAS, 314, 65
Lucy, L. B. 1984, ApJ, 284, 351
Lucy, L. B., & White, R. L. 1980, ApJ, 241, 300
Malkov, M. A. 1998, Phys. Rev. E, 58, 4911
Malkov, M. A., & Völk, H. J. 1995, A&A, 300, 605
Malkov, M. A., & Völk, H. J. 1998, Adv. Space Res., 21, 551
McKenzie, J. F., & Völk, H. J. 1982, A&A, 116, 191
McClements, K. G., Dendy, R. O., Bingham, R., et al. 1997, MNRAS, 291, 241
Ratkiewicz, R., Axford, W. I., & McKenzie, J. F. 1994, A&A, 291, 935
Reynoso, E. M., Moffet, D. A., Goss, W. M., et al. 1997, ApJ, 491, 816
Scholer, M., Trattner, K. J., & Kucharek, H. 1992, ApJ, 395, 675
Trattner, K. J., & Scholer, M. 1994, JGR, 99, 6637
Völk, H. J. 1984, in Proc. 19th Rencontres de Moriond, Astrophysics Meet. High Energy Astrophysics, ed. J. Tran Thanh Van (Gif-sur-Yvette: Éditions Frontières), 281
Völk, H. J. 2001, to be published in Proc. 26th Rencontres de Moriond, Very High Energy Phenomena in the Universe, Les Arcs [astro-ph/0105356]
Völk, H. J., Berezhko, E. G., Ksenofontov, L. T., & Rowell, G. P. 2002, A&A, 396, 649